

Babinet's principle in the Fresnel regime studied using ultrasound

Akira Hitachi^{a)} and Momo Takata

Kochi Medical School, Nankoku, Kochi 783-8505, Japan,

The diffraction of ultrasound by a circular disk and an aperture of the same size have been investigated as a demonstration of Babinet's principle in the Fresnel regime. The amplitude and the phase of diffracted ultrasonic waves have been measured and a graphical treatment of the results is performed. The results verify Babinet's principle. It is also found that the wave without the diffracting objects is indeed 90 deg in phase behind the wave from the center of the zone system. This paradox has previously been regarded as a defect of Fresnel's theory.

Keywords: Babinet's principle, Poisson's bright spot, Fresnel diffraction, ultrasound

I. INTRODUCTION

The phenomenon of Poisson's bright spot (the spot of Arago)^{1,2} can be used to gain the attention and interest of not only students of physics but also of those of general science classes. The high intensity spot just behind a circular opaque obstacle arouses curiosity. The addition of observation of the complementary circular aperture, provides quantitative measurements on the mathematical theory of waves. With ultrasound measurements the essence of the theory can be seen by simply drawing vectors in the complex plane, without complicated calculation. The apparatus is inexpensive and can be made by hand. The measurement is as simple as learning how to use the oscilloscope.

A general description of Babinet's principle states that the sum of the diffraction fields U_1 and U_2 behind two complementary objects is the field U_0 observed without the diffracting objects.³⁻⁷

$$U_0 = U_1 + U_2 \quad (1)$$

This principle is generally fulfilled within the framework of the scalar theory of diffraction.⁷ Verification of the Babinet's principle has been almost exclusively performed with light. The diffracted patterns ($I = UU^*$) are compared in the Fraunhofer regime (source and observation plane situated very far from the diffracting object). In the Fresnel regime (source and observation plane at a finite distance from the diffracting

object), the patterns are compared through calculation.¹ It is mainly because the wavelength is too short and the frequency too high to observe the phase. In microwave region, the wavelength becomes a few cm. It is possible to make use of this advantage, e.g. the phase dependence of the dielectric transient absorption allows observation of a phenomenon several orders of magnitude faster than the time resolution which is determined by the Q value of the cavity.⁸ The wavelength of ultrasound is also several mm and the period is a few tens of microseconds. Then, it is possible to manipulate and observe the phase as well as the amplitude. This enables Babinet's principle to be studied directly comparing the amplitude and the phase.

We will observe diffraction by a circular aperture having diffracted field U_a and a complementary circular disk U_d and study Babinet's principle, $U_0 = U_a + U_d$, by using ultrasound. The regime investigated by ultrasound can be somewhat different from the usual Fresnel or Fraunhofer regimes observed by light. In most theory and measurements with light, an opaque object is required to be much larger than the wavelength, and its size is also to be much smaller than its distances from the source and screen. In the present case, however, the objects sizes are only 10 times the wavelength and the distances are only a few times the objects. It will be complicated to construct the theory. In the present paper, graphical treatment is used to analyze observed amplitude and phase.

Since the wavelength of the ultrasound is long the diameter of the first Fresnel half-period zone can be several cm. Therefore it is possible to observe effects to within a small fraction of the half-period zone. The vibration spiral for the circular aperture can be investigated in detail.

II. GRAPHICAL TREATMENT OF DIFFRACTION WITH CIRCULAR OBJECT

A graphical treatment, based on Huygens-Fresnel diffraction theory, gives a clear physical picture of the origin of the diffraction pattern.^{3,5,6} We consider the field diffracted by a circular aperture at point P on the axis. A point source is placed on the axis distance z_0 from the aperture. We consider a series of spheres centered at P of radius $z + \lambda/2$, $z + 2\lambda/2$, $z + 3\lambda/2$ and so on, differing by $\lambda/2$. Their intersections with the spherical wave front at the aperture form circular zones. The zones are called Fresnel or half-period zones. The phases between zones differ by π . Fig. 1a shows the amplitude diagram in the complex plane when the first half-period zone is divided into eight subzones.³ The vector a_1 represents the contribution from the first subzone. The

amplitudes a_2 and a_3 due to the second and third subzones are added. The phase difference δ between each successive one will be $\pi/8$. Adding all eight subzones gives the vector OG as the resultant amplitude from the first half-period zone. Similarly, the contribution from the second half-zone is GH , and OH is the sum of the first two zones. Succeeding half-period zones give the rest of Fig. 1a. Increasing the number of subzones indefinitely, the vibration spiral is obtained as shown in Fig. 1b. U_a is represented by vector OD . The spiral eventually approaching C the half-period zone cover the whole spherical wave, i.e., U_0 is represented as the vector OC . In Babinet's principle, $U_0 = U_a + U_d$, where U_d is DC . The argument here also applies for the plane wave geometry.

The spiral also allows one to determine directly the resultant amplitude and the phase due to any fractional number of zones. The phase can be estimated by simply calculating Δ_B , the difference between the path length along the axis and that via the edge of the circular object. The angle φ ($\angle OCD$) seen from the center of the spiral and starting on point O is given by $2\pi \times \Delta_B / \lambda$.

Fig. 1 applies for the time $t = 0$. The vectors revolve clockwise with the same angular velocity ω . The triangle representing U_0 , U_a and U_d revolves as a rigid frame. The simple harmonic wave is presented as the projection on the coordinate of the real part. We adopt here the custom in optics of representing an advance of phase by a clockwise rotation of the amplitude vector.

One other problem arises. The resultant vector U_0 turns out to be $\pi/2$ in phase behind the wave from the center of the zone system.^{3,6} The paradox has been regarded as a defect of Fresnel's theory resulting from the approximations made therein.

III. EXPERIMENTAL METHOD

The experimental arrangement using ultrasound is shown schematically in Fig. 2. The transmitter T (Nicera T4016) was driven at 40 kHz by an oscillator. This gives a wavelength λ of 8.58 mm at room temperature. The frequency was monitored by a frequency counter. The transmitter and the center of the diffracting objects were placed on the axis so that the ultrasonic path has cylindrical geometry about the normal to the object through its center. The receiver R (Nicera R4010A1) was chosen because it has a wide signal accepting angle (110° FWHM) and was set on a rail placed perpendicular to the axis and scans the radial distribution of the signal beyond the circular aperture or a disk. The distances z_0 and z are from the diffracting object (the aperture or the disk) to

the source and the scanning line respectively. A transmitter with narrow emitting angle (50 °FWHM) was chosen in order to avoid undesirable reflection mainly from the table. The distance z_0 was set to be larger than z in order to use a relatively uniform sound pressure at the front of the transmitter. The signal from the receiver was put into ch1 of an oscilloscope and the power to the transmitter was monitored in ch2. The power levels were 2 - 4 V_{p-p} . Then the amplitude of the receiver and the phase difference to the signal in ch2 were observed. The amplitude and the phase were registered as a function of the radial distance r . The diameters of the transducers were 7 mm and 6 mm for T4016 and R4010A1, respectively

A. Circular aperture and disk

The receiver was put on a rail placed 858 mm from the transmitter. The complementary circular aperture or disk was placed 146, 226 and 326 mm from the receiver. These arrangements give $(z_0+z) = 100\lambda$ and $z = 17\lambda, 26.3\lambda$ and 38λ , respectively, at room temperature. The position on the vibration spiral can be changed by changing z . These arrangements give $\Delta_B = (Z_0+Z)-(z_0+z)$ of $0.87\lambda, 0.64\lambda$ and 0.53λ which corresponds to $\varphi = 2\pi\Delta_B/\lambda = 313, 230$ and 190 deg, respectively,

A circular aperture of 8.6 mm (10λ) in diameter cut into 0.6 mm thick hard paper was placed on a cork board of 900 mm wide, 600 mm high and 6mm thick with a circular hole of 118 mm ϕ . A circular disk of the same diameter which was supported by a carbon rod of 4 mm ϕ was also prepared. The disk was backed by a circular cork disk of 69 mm ϕ and 4 mm thick. The heights of the centers of the transmitter, the receiver, the aperture and the disk were set to be 340 mm.

B. Small aperture

A small aperture, which will contain only a tiny fraction of a half-period zone, was prepared. The phase difference between with and without the aperture was measured. We used an aperture of $1.4\lambda\phi$ and used the graphical treatment. A4 size paper of 0.6 mm thick with a 12mm ϕ hole at the center was placed on the aperture described above. The fraction of half-period zone covered was changed by altering the position of the small aperture. The aperture was set between $z = 17\lambda - 38\lambda$. The fraction can be as small as 1/30 - 1/50 half-zone. The phase and the amplitude between with the small aperture (as a_1 in Fig. 1) and without (vector OC) were compared on the axis. The phase was also observed off the axis as a function of radial distance.

IV. RESULTS

The relationship between U_0 , U_a and U_d for the $10\lambda\phi$ aperture and the disk placed 17λ , 26.3λ and 38λ , from the receiver set on the axis are shown in Fig 3. The end points for vectors U_a and $U_0 - U_d$ are plotted as open and closed symbols. The phase θ_0 for no diffracting object was assumed to be $\pi/2$. The distance between the transmitter and the receiver was 100λ . The ϕ values calculated by the path difference Δ_B for each arrangement are shown with bars on the circle. The aperture contains less than two half-period zones with these arrangements. The scattered points are results for different runs. The arrows show the average values. The main contribution to the error comes from errors in the phase. The amplitude for U_d is observed larger than that for U_a and points are mostly outside the circle except for 17λ . On the other hand, most points for U_a lay inside of the circle. The reason may be due to the finite thickness of the edges, limited radial width of incident ultrasound, and errors in alignment. Although, there still are small discrepancies in points for U_a and U_d , the agreement between the graphical treatment and experimental results is quite good. It has also been shown that the point moves counter clockwise on the spiral as Δ_B increases when the objects approached from the center to the receiver. The position on the vibration spiral can be selected by changing the position z of the diffracting object.

Similar measurements were also performed for off the axis positions. The vectors representing U_0 , U_a and U_d off the axis do not lie on the circle. However, they make a triangle as expected by Babinet's principle.

The typical radial diffraction patterns, the amplitude A and the phase θ , obtained for U_0 , U_a and U_d are shown in Fig. 4. The amplitude patterns for aperture A_a and disk A_d are quite different from each other and one cannot tell the relation by just looking at those patterns. However, Babinet's principle is clear when one compares the amplitudes and phase, either on or off the axis as mentioned above.

There are five characteristic positions shown in Fig. 4. One is the axis, and two are geometrical edges (vertical broken lines) which lay symmetrically to the axis. Other positions M_1 where all phases come close (dot-dash lines). The phases also come close to each other at the geometrical edges where A_0 is nearly equal to $A_a + A_d$ as expected by Babinet's principle. These points in the position differ slightly each other. The difference may be due to the finite size of the receiver.

A_0 and θ_0 change smoothly as expected over the whole range observed. Observed A_0 values are fairly flat and nearly constant. The parabolic curve shows the phase change calculated by the difference in transmitter-receiver distance between on the axis

(z_0+z) and radial position (TR') for no aperture. Observed θ_0 agrees well with the calculated curve.

Generally, θ_a changes smoothly except on the axis and near position M_1 . A_a almost vanishes at M_1 and the phase flip was observed. The A_d pattern has also a small minimum at M_1 . Such points appear again farther out. A_a increases slowly when approaching the geometrical edge from outside. However, the phase θ_a changes rapidly in the geometrical shadow. Two maxima lay symmetrically to the axis inside the geometrical edges. Change in θ_a becomes slow inside the edge, except in the vicinity of the center. A_a and θ_a on the axis change as the position z of the aperture changes. A_a can be between 0 and twice A_0 depending on z . In present arrangements, two A_a maxima were observed at around $z = 44\lambda$ and 56λ . A_a was observed to be about $1.9 A_0$ and θ_a was nearly equal to θ_0 at the maximum. An A_a minimum was observed at $z = 14\lambda$. θ_a changed abruptly from behind to ahead of θ_0 as the aperture approaching the receiver in the vicinity of the minimum.

On the other hand, the A_d is almost constant and the same as A_0 , except near M_1 , till it approaches the geometrical shadow, then it starts decreasing. Structures appear inside the geometrical shadow. Poisson's bright spot appears on the axis surrounded by small maxima. The phase θ_d is almost the same as θ_0 outside the geometrical shadow. Inside the shadow, the phase goes behind and reaches nearly 2π behind θ_0 on the axis. The θ_d change in the vicinity of minima is quite large. θ_d on the axis differs by nearly 2π from θ_0 with this arrangement. One cannot tell the difference by only looking at phases for θ_d and θ_0 near the axis. However, the difference is clear by observing over a wide range. This is also seen in the vibration spiral as shown in Fig. 3 where U_d has rotated nearly 2π .

The radial position M_1 where the phase θ_a starts the reversal movement corresponds to eclipse of the half-period zones. When the observation point P moves out from the center and goes into the geometrical shadow, the Fresnel zone system follows. As P moves further, the total eclipse of a half-period zone occurs, the phase θ_a goes ahead instead of behind near this point. A_0 is small and the changes in A_0 are not evident in this region.

The amplitudes and phases obtained for the $12 \text{ mm}\phi$ aperture are plotted on a vibration spiral as shown in Fig.5. The distance between the transmitter and the receiver was 100λ , the same as before. The small aperture was set at $z = 17\lambda$, 26.3λ and 38λ , which give Δ_B values of 0.017λ , 0.013λ and 0.010λ , respectively. The figure shows the resultant vector OC is indeed to be nearly 90 deg in phase behind the wave from the vector due to a very small aperture.

The radial diffraction patterns for the amplitude A_{s1} obtained for a small aperture at $z = 17\lambda$ is shown in Fig. 6 together with A_0 . A broad peak with a small structure at the center was observed for A_{s1} . The amplitude on the axis is almost 1/10 that observed for no aperture. The phase θ_{s1} and θ_{s3} observed at $z = 17\lambda$ and 38λ , respectively, are also shown in Fig. 6. The phase difference between the path via the center of the aperture and via the edge was quite small. Only a tiny fraction of a half-period zone appears in the small aperture, close to Fraunhofer diffraction. Parabolic curves are phase differences calculated for the geometrical path difference between the source to the point on the axis (z_0+z), and the source to the observation position via center of the aperture (z_0+OR'), added a phase differences of -75° or -90° . The measured phase difference agrees fairly well with either of the curves. It is clearly seen that the wave due to a small aperture on the axis is indeed $\pi/2$ ahead in phase than the wave with no aperture as expected with Fresnel diffraction.

V. DISCUSSION

This experiment is in the extreme Fresnel regime in the sense that the diffracting object is not very small compared with the distances z_0 and z . The angles θ_η and θ'_η , the incident and diffracted wave would make, are quite large. In another sense, it is close to the Fraunhofer regime; in spite of a large aperture and a short distance z , the total number of zones involved is quite small, in fact can be less than 2.

Lommel developed a special formulation of the Kirchhoff theory suitable for a circular aperture and a disk. The diffraction patterns for the circular aperture and disk are given by Lommel functions, which is described in terms of the first Bessel functions. The amplitudes and positions for peaks and trough may be described by Lommel functions.¹ We consider for simplicity the diffraction on the axis.

Fresnel-Kirchhoff diffraction for a point source and a circular aperture in polar coordinates can be expressed in terms of the no aperture field $U_0(P)$. One obtains for point P on the axis,⁵

$$U_a(P) = -iU_0(P) \int_0^{\varphi_0} e^{i\varphi} Q(\varphi) d\varphi \quad (2)$$

$$U_0(P) = A_{na} \exp\{-i(\omega t - kr + \theta)\}/r \quad (3)$$

where φ_0 is the value of the phase difference at P between a wave that comes from the edge of the aperture and that which follows the z -axis. The $-i$ appears in Eq. (2) means that the diffracted wave is $\pi/2$ ahead in phase. It is customary in optics to represent an

advance of phase by a clockwise rotation of the amplitude vector as mentioned previously. The phasor integral

$$I(\varphi_0) = \int_0^{\varphi_0} Q(\varphi) e^{i\varphi} d\varphi \quad (4)$$

gives the vibration spiral as shown in Fig. 1b. The inclination factor $Q(\varphi) = \frac{1}{2}(\cos\theta_\eta + \cos\theta'_\eta)$ is a smooth monotonically decreasing function. θ_η and θ'_η are angles that diffracted wave would make with a unit vector perpendicular to the diffraction plane. For a few turns $Q(\varphi)$ is close to 1. Therefore, the spiral may be regarded as a circle. $I(\varphi_0) = 1+i, 2i, -1+i$ and 0 for $\varphi_0 = \pi/2, \pi, 3\pi/2$ and 2π , respectively, as shown in Fig. 1b. In the limit of infinite aperture radius, $I(\varphi_0)$ becomes i , and $U(P)$ approaches $U_0(P)$, the incident wave. The resultant phase from Eq. (2) is $-\pi/2$ for a wave that follows the z axis and 0 for no aperture. The vibration spiral in Fig. 1 should be turned 90° clockwise, then U_0 is on the real axis. The graphical treatment does not have i which appears in Eq. (2) and give the paradox that the incident wave has a $\pi/2$ delay in phase.

The diffracted field for the plane wave by a circular aperture along the axis is given by Rayleigh-Sommerfeld diffraction theory as follows,^{9,10}

$$U_a(z) = A_{na} z \left[\frac{\exp(ikz)}{z} - \frac{\exp(ikZ)}{Z} \right] \quad (5)$$

where $Z = \{z^2 + (D/2)^2\}^{1/2}$ is the distance between the edge and the observation point on the axis. This surprisingly simple formula is an exact expression for the scalar field and valid anywhere along the axis. It should be noted that an edge-diffraction calculation⁹ and a conventional two-dimensional integration over the area of the aperture¹⁰ yield the same result. The first term is the incident plane wave $U_0(z)$ and consequently the second term is $U_d(z)$.

An edge diffracted approach by Young and a secondary wavelet approach by Huygens-Fresnel are two fundamental physical models of diffraction.^{4,11} The two approach are considered as equivalent mathematical treatments as shown in Eq. (5). An edge diffracted approach states the field behind the object as the superposition of the incident wave and the boundary diffraction wave (U_B , wave originated at the edge) in the illuminated region, and the boundary diffraction wave in the geometrical shadow. In the approximations of the Kirchoff theory,⁴

$$U_a(r) = A_{na} \frac{\exp(ikr)}{r} + U_B(r), \quad P \in J \quad (6)$$

$$U_a(r) = \quad \quad \quad + U_B(r), \quad P \notin J \quad (7)$$

Then on the axis, we have $U_B = -U_d$ in Eq. (5).

Now we move into the Fresnel regime ($z \gg a$) and look at $U_d(z)$ as a function of D at a fixed z on the axis. The amplitude is given by $z/Z \cdot A_{na}$ with Eq. (5) and is almost equal to A_{na} when D is not too large. The phase difference from the incident wave is given by $\varphi = 2\pi\Delta/\lambda = 2\pi(Z-z)/\lambda$. Let us put the endpoint of vector U_d onto that of U_0 and see the trace of the starting point of U_d , which is also the end point of U_a , on the complex plane by changing D . Fresnel zones can be obtained as $z + \Delta = z + n \cdot \lambda/2$. Then we have the vibration spiral as shown in Fig. 1b, except U_0 is on the real axis.

Next, we consider a very small aperture. U_0 and U_d become close and U_B has the phase change⁴ π to the incident wave U_0 for P on the axis according to Eq. (5). Therefore, the sum vector U_a becomes $\pi/2$ ahead from U_0 as the present measurement shows. When P moves in to the shadow, U_0 vanishes and only U_B remains. Then, U_a should have the phase difference of π in the shadow. However, the phase difference for U_a remains $\pi/2$ both on the axis and in the geometrical shadow as shown in Fig. 6. One of the reasons may be due to the approximations^{4,12} made in deriving Eqs. (6) and (7).

When the point source and observation point is fixed, the phase is simply predicted by the path difference between the wave along the axis and the wave via the edge of the aperture independent of the position of the aperture or the disk. The wave observed for a small aperture, which contains only a fraction of a half-period zone, is always $\pi/2$ ahead in phase than the wave without the aperture, provided that the aperture is small enough and is not too close to the source or the observation point.

The apparatus used is far from ideal. It was intended as a table-top apparatus for the student laboratory. However, it is still capable of showing fundamental aspects of the theory of diffraction. Ideally one needs a uniform wave and a huge room with no reflection to investigate more closely the wave theory including the phase. In the classroom, however, satisfactory results can be obtained by setting the transmitter and the receiver close to each other with a proper alignment. Since Babinet's principle can be studied directly, the diffracting object needs not to be circular. An elliptical form or squares, in fact any form can be used. The method may also be related in mathematically, introducing 'the most remarkable formula in mathematics' (R.P. Feynman), Euler's Formula: $e^{i\theta} = \cos\theta + i\sin\theta$ and the complex plane.

V. CONCLUSIONS

Babinet's principle in the extreme Fresnel regime has been confirmed directly by observing ultrasound waves diffracted by a circular aperture and a complementary disk.

The phase as well as the amplitude was observed and analyzed by a graphical treatment. It has been also found that the wave without the diffracting objects is indeed 90 deg in phase behind the wave from the center of the zone system. The paradox has been regarded as a defect of Fresnel's theory. The $\pi/2$ phase difference appears also in Fresnel-Kirchhoff diffraction, Rayleigh-Sommerfeld diffraction and even in the edge-diffracted approach by Young.

ACKNOWLEDEMENTS

The authors would like to thank researchers of Kitasato University for a valuable discussion. We are also grateful to Prof. T. A. King of Manchester University for reading of the manuscript.

References

- ^{a)}Electronic address: jm-hitachia@kochi-u.ac.jp
- ¹P. M. Rinard, "Large-scale diffraction patterns from circular objects" *Am. J. Phys.* 44, 70-76 (1976).
- ²J. E. Harvey and J. L. Forgham, "The spot of Arago: New relevance for an old phenomenon" *Am. J. Phys.* 52, 243-247 (1984).
- ³F. A. Jenkins and H. E. White, *Fundamentals of Optics* (McGraw-Hill, New York, 1957), 3rd ed.
- ⁴M. Born and E. Wolf, *Principle of Optics* (Pergamon, Oxford, 1980), 6th ed.
- ⁵M.V. Klein and T. E. Furtak, *Optics* (John Wiley & Sons, NY, 1986), 2nd ed.
- ⁶E. Hecht, *Optics* (Addison-Wesley, Reading, 1987), 2nd ed.
- ⁷J. R. Jiménez and E. Hita, "Babinet's principle in scalar theory of diffraction" *Opt. Rev.* 8, 495-497 (2001).
- ⁸F. W. Fessenden and A. Hitachi, "A study of the dielectric relaxation behavior of photoinduced transient species" *J. Phys. Chem.* 91, 3456-3462 (1987).
- ⁹A. Dubra and J. A. Ferrari, "Diffracted field by an arbitrary aperture," *Am. J. Phys.* 67, 87-92 (1999).
- ¹⁰J. E. Harvey and A. Krywonos, "Axial irradiance distribution throughout the whole space behind an annular aperture: reply to comments," *Appl. Opt.* 42, 3792-3794 (2003).
- ¹¹S. Ganci, "An experiment on the physical reality of edge-diffractive waves," *Am. J. Phys.* 57, 370-373 (1989).
- ¹²G. D. Gillen and S. Guha, "Modeling and propagation of near-field diffractions: A more complete approach," *Am. J. Phys.* 72, 1195-1201 (2004).

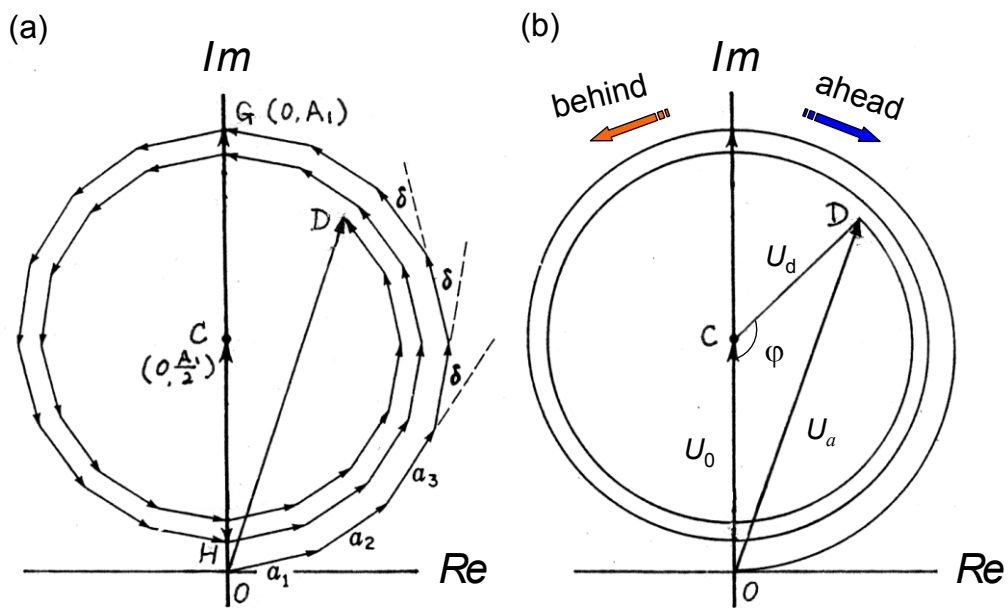


Fig. 1. Vibration spiral for Fresnel half-period zones of a circular aperture.
 (a) half-period zones are divided into 8 subzones,
 (b) indefinite number of subzones.

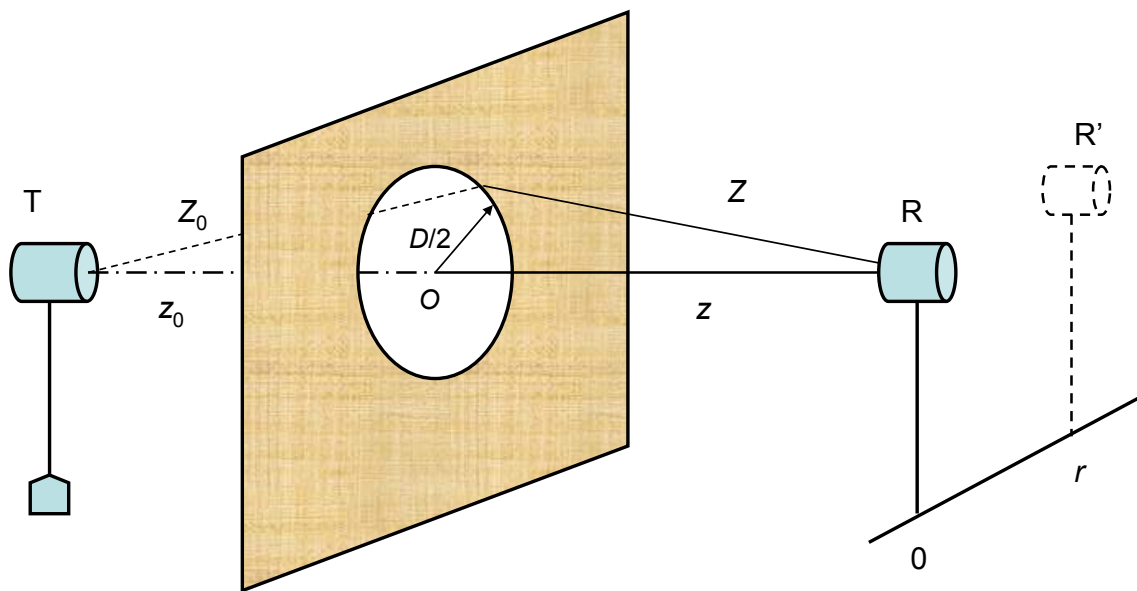


Fig. 2. Schematic view of arrangement for the experiment with a circular aperture.

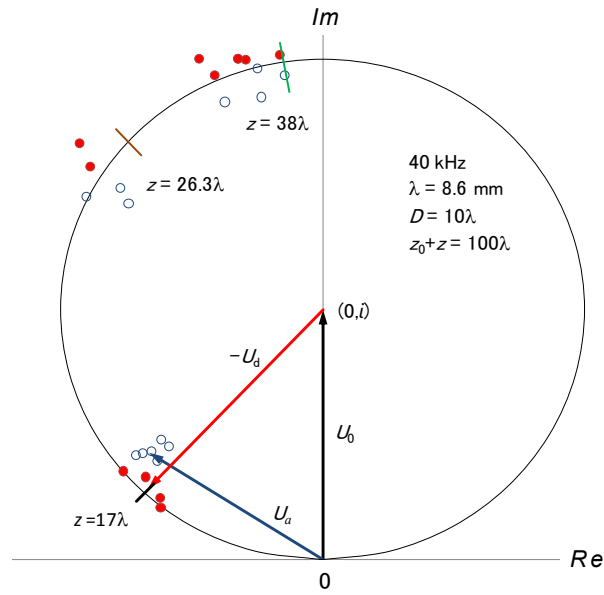


Fig. 3. The amplitude and phase relation obtained for no aperture U_0 , a circular aperture U_a and a circular disk U_d . The receiver was set on the axis. The phase θ_0 for U_0 was taken to be $\pi/2$. The end points for vectors U_a and $U_0 - U_d$ are plotted with open and closed symbols, respectively.

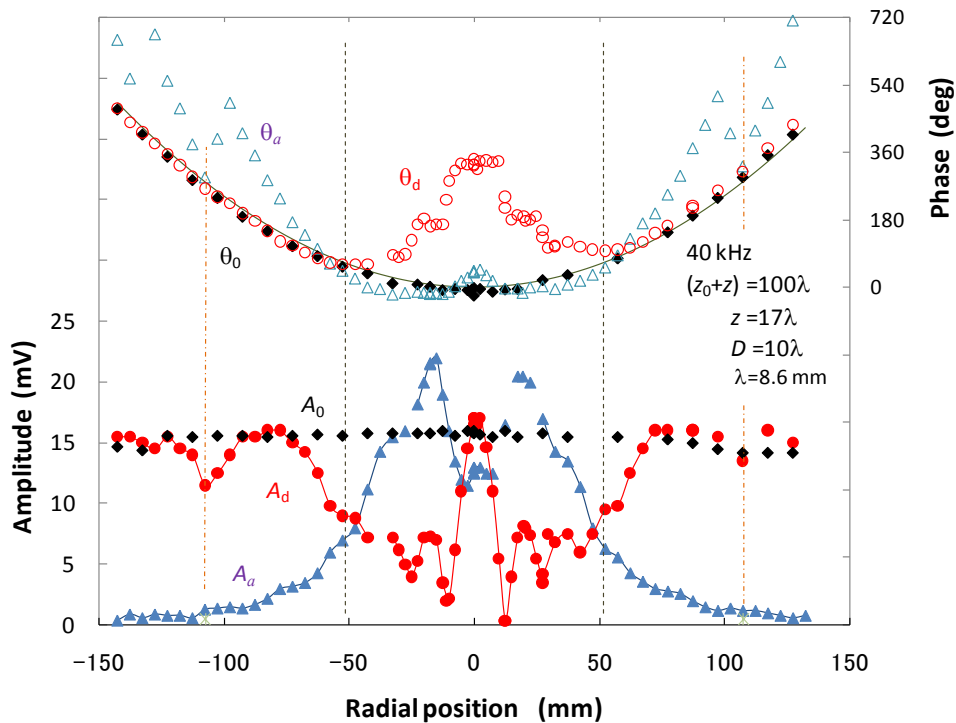


Fig. 4. The diffraction patterns for the amplitude A (lower) and the phase θ (upper) as a function of the radial distance r from the axis observed for complementary circular aperture and disk.

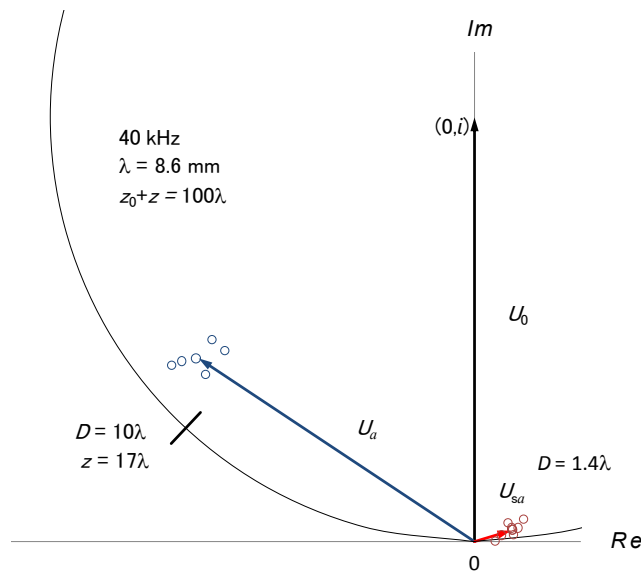


Fig. 5. The amplitude and phase relation obtained for a small aperture (U_{sa}) of $1.4\lambda\phi$. The receiver was set on the axis. The distances z are 17λ , 26.3λ or 38λ . The points obtained for an aperture (U_a) of $10\lambda\phi$ are also show for comparison.

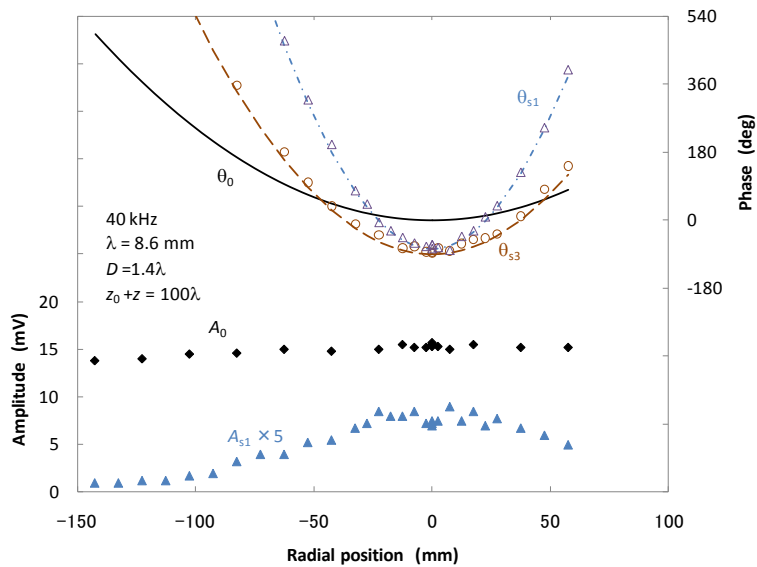


Fig. 6. The diffraction patterns for the amplitude A (lower) and the phase θ (upper) as a function of the radial distance observed for a small aperture of $1.4\lambda\phi$. 1 and 3 stand for the distances z is 17λ and 38λ , respectively. Parabolic curves are phase differences calculated for the geometrical path difference between the source to the point on the axis, and the source to the radial position r via center of the aperture added with -75° or -90° .